"BABEŞ-BOLYAI" UNIVERSITY

FACULTY OF PHYSICS

Baidoc Sergiu Cristian

Study of some structural and physical properties of some B_2O_3 based glasses containing Ag_2O and 3d ions

Ph.D Thesis Summary

Scientific supervisor

Prof. Univ. Dr. Ioan Ardelean

Cluj-Napoca

2011

Table of contents

Introduction

Borate glasses are very interesting due to the presence of the phenomenon of so called „boron anomaly" which consists of forming of boron tetrahedral structural units (BO_4) beside the tri-coordinatd ones which exits in pur vitreous B_2O_3. These glasses have a low commercial importance because of their degradation in contact with the water from the atmosphere. Their analysis is still important because their structure and properties which are different from silica based glasses, knowing the fact that very important economic category is represented by borosilicate glasses.

Also, the presence in diamagnetic vitreous matrices of 3d transitional metal ions determinates a different magnetic behavior which depends from the concentration of these ions, from their valence state, from their distribution in matrix and the nature of the glass.

The structural and physics properties invstigations of B_2O_3 based glasses with 3d ions tries to ascertain from fundamental point of view the role played by the transitional ions in establishing the properties of these glasses and to determine the physics mechanisms that stand at the base of these properties.

In this ideea, there have been prepared and investigated the next vitreous systems: $xAg_2O\cdot(100-x)[zB_2O_3\cdot As_2O_3]$ with $0 \leq x \leq 10$ mol% and z = 1; 2; 3 and $x[(1-y)Ag_2O\cdot yMnO]\cdot(100-x)[2B_2O_3\cdot As_2O_3]$ with x = 10 mol% and $0 \leq y \leq 50$ mol%. In order to obtain these information the next investigation methods were used: X – ray Diffraction, FT – IR spectroscopy, Raman spectroscopy, electron paramagnetic resonance (EPR) and magnetic susceptibility measurements. The results obtained have allowed the pursue of the structural changes, by varying the silver ions content, and the magnetic properties which appear in these glasses by varying the manganese ions content.

The study presented in this thesis has as objective the obtaining of new experimental data and the clarification of the physical phenomenon's which determine the structural behavior of B_2O_3 based glasses doped with silver and manganese ions.

The thesis is structured in four chapters.

In the first chapter are presented, on literature basis, the main results regarding the structure and the properties of B_2O_3 based glasses. The second chapter presents theoretical aspects about the study methods used in the determination of the structural and magnetic properties of the investigated glasses. In the third chapter are presented information regarding the preparation mode of the investigated glasses and also the experimental techniques used. In the forth chapter are presented and disscused the experimantal results obtained for the investigated glasses. In the end are presented the general conclusions which evidenced the most important results of this thesis.

Keywords: *glasses, x-ray Diffraction, FT – IR spectroscopy, Raman spectroscopy, EPR, magnetic susceptibility, manganese ions.*

Chapter I

Structure of B_2O_3 based glasses

The common oxidic glass is known fron the antiquity, being used as constructions material, as art objects, as adornments, as electronic materials , as biomaterials, absorbent shield in nuclear technique, in photographic technique, etc., with applicability in so many other domains.

Oxidic glasses are a part of non-crystalline solid materials in which the atoms are disposed in a way similar to the crystals, but their arrangement is not regular, presenting only local order. In order to obtain glasses there is a large number of oxide species known as vitreous network forming (SiO_2, B_2O_3, P_2O_5, GeO_2, TeO_2, V_2O_5, Bi_2O_3, etc.). The other oxides which enter in the chemical composition of the glasses, stabilizing it and modifying its properties have been named vitreous network modifier or stabilizer oxides (K_2O, CaO, Na_2O, CdO, SrO, Li_2O, etc.).

In crystalline state, B_2O_3 presents a hexagonal simetry structure with $P3_1$ (C_3^2) spatial group, with network parameters c = 8,317 Å and a = 4,325 Å [1,2]. Also, it is considered that in crystalline state boron has in the first coordination sphere three oxygen atoms that are arranged in a planar configuration of equilateral triangles with sides of 2,40 Å. The boron atom is in the middle of the triangle with B-O distance of triangles 1,38 Å, and the bonds angle O-B-O of approximately 120^o. The triangles are connected through peaks that form chains.

The angle formed by two oxygen bridges is 168^o. Admitting the multi-layer structure of crystalline boron oxide, it's expected to find these chains even in melts. The experimental data shows that the B-O-B bond's energy in chains and in cycles is the same, forming a cycle requires only bonds angle's modification. Above certain temperature, by breaking some chain bonds, boroxol cycles are formed which disappear at temperatures above 800^oC.

Adding different modifiers (PbO, Na_2O, K_2O, etc) in B_2O_3 glasses, it can be obtain binary glasses in which the modifier determines structural changes, complicating even more the structure of these glasses [3-5]. The increasing of alkaline oxide concentration determines not only the

increasing of boron coordination, but also the breaking of dome oxygen bridges which leads to depolimerization.

The introduction of a third component in B_2O_3 based glasses complicates even more the structure of these glasses and the investigation of their structure and properties. Analizing the structure of ternary borate glasses is more complicated than binary borate glasses and starts with analizing th structure of the binary borat glasses. In this paper the components which are present in chemical composition of borat glasses are Ag_2O and MnO.

The introduction of transitional metal ions the glasses special electrical and magnetical properties and at the same time they are used as check rod for investigating the structure of these glasses.

Examples of ternary systems that contains Ag_2O and MnO with B_2O_3 as network formative which have been investigated from the structural point of view (through FT-IR and Raman spectrosopies and through electron paramagnetic resonance, EPR) and from the physical properties point of view (through magnetic susceptibility or electrical conductivity measurements) are : MnO-B_2O_3-Na_2O [6], MnO-B_2O_3-K_2O [7], MnO-B_2O_3-As_2O_3 [8], CuO-B_2O_3-Ag_2O [9], CuO-MnO-B_2O_3-K_2O [10], etc.

Chapter II

Theoretical and experimental aspects regarding the use of some study methods of oxide glasses based on B_2O_3 structures and properties

Studying oxidic glasses with transitional metal ions has as ajective the gathering of information regarding their structure and their properties, in order to contribute in the elaboration of vitreous solid theory and finding new practically applications. The investigation methods used for this study are X – ray diffraction, FT – IR spectroscopy, Raman spectroscopy, electron paramagnetic resonance (EPR) and magnetic susceptibility measurements.

X – Ray diffraction is the most used investigation method in order to establish if a material is crystalline, vitreous or amorphous. In order to do this you have to obtain the X-ray diffraction image and to know how the destruction of crystalline state affects the diffraction image.

FT – IR spectroscopy is used in crystalline and in non-crystalline materials studies, being one of the most used methods for investigating the molecular structure and for qualitative and quantitative analysis of substances. The structure of the IR absorption spectrum gives us information regarding the geometrical properties of the molecule (distances between atoms, valence angles, and force constants) and its chemical structure.

The Raman spectroscopy, complementary to IR spectroscopy, brings useful contributions to the molecular vibrations study. Comparing with FT-IR spectra, the Raman spectra has a number of advantages : the bands are, generally, well-defined; limited in numbers and often polarized; they have a strong dependence of composition; with a small sensibility to surface contamination and water content; the samples permit volume effects measurements; measuring at high temperatures is a lot easier.

EPR is a method widely used to describe the fundamental states and to characterize the vicinities effect on the energetic levels of the paramagnetic centers. The EPR is a sensitive method in detecting atoms position in the structure and in studying the local symmetry. The method consist in the study of the electronic levels split of the atoms in the presence of an extern magnetic field.

In oxide vitreous systems you will not encounter all types of magnetic order as in crystalline solid materials [11]. The presence in diamagnetic vitreous matrices of transitional metal ions determines different magnetic behaviors, which depend on the concentration of these ions, on their valence state and on the structure of the glass. The presence of isolated magnetic ions in vitreous matrices have been evidenced also through paramagnetic resonance electron measurements. The magnetically properties of these glasses are generally given by the paramagnetic ions, the characteristics of the base glass being only a small factor in its properties.

Chapter III

Experimental techniques

The raw materials used in the preparation of the investigated glasses are: $AgNO_3$, H_3BO_3, As_2O_3 and $MnCO_3$. These materials were mixed in stoechiometric proportions given by chemical

formula for $xAg_2O\cdot(100-x)[zB_2O_3\cdot As_2O_3]$ with $0 \leq x \leq 10$ mol% and z = 1; 2; 3 and $x[(1-y)Ag_2O\cdot yMnO]\cdot(100-x)[2B_2O_3\cdot As_2O_3]$ with x = 10 mol% and $0 \leq y \leq 50$ mol% and melted at 1200 ˚C in aluminum crucible for a half an hour to achieve better homogenization. In order to obtain a vitreous structure, the melt was cooled on a plate of stainless steel (melt cooling method).

The structure of samples was analyzed by means of x-ray Diffraction, using powders, with a Philips X´Pert MPD diffractometer. For reference it was used JCPDS – International Center for Diffraction Data base. To confirm the data obtained from these measurements was also used the scanning electron microscopy method.

In order to confirm the vitreous state in $xAg_2O\cdot(100-x)[zB_2O_3\cdot As_2O_3]$ with $0 \leq x \leq 10$ mol% and z = 1; 2; 3 – (a) ; (b) ; (c) ; (d) and $(1-y)Ag_2O\cdot yMnO\cdot 9[2B_2O_3\cdot As_2O_3]$ with $0 \leq y \leq 50$ %mol (e) systems X-Ray diffraction measurements have been made. Most significant X-ray difractograms are presented in figure III.1.1.

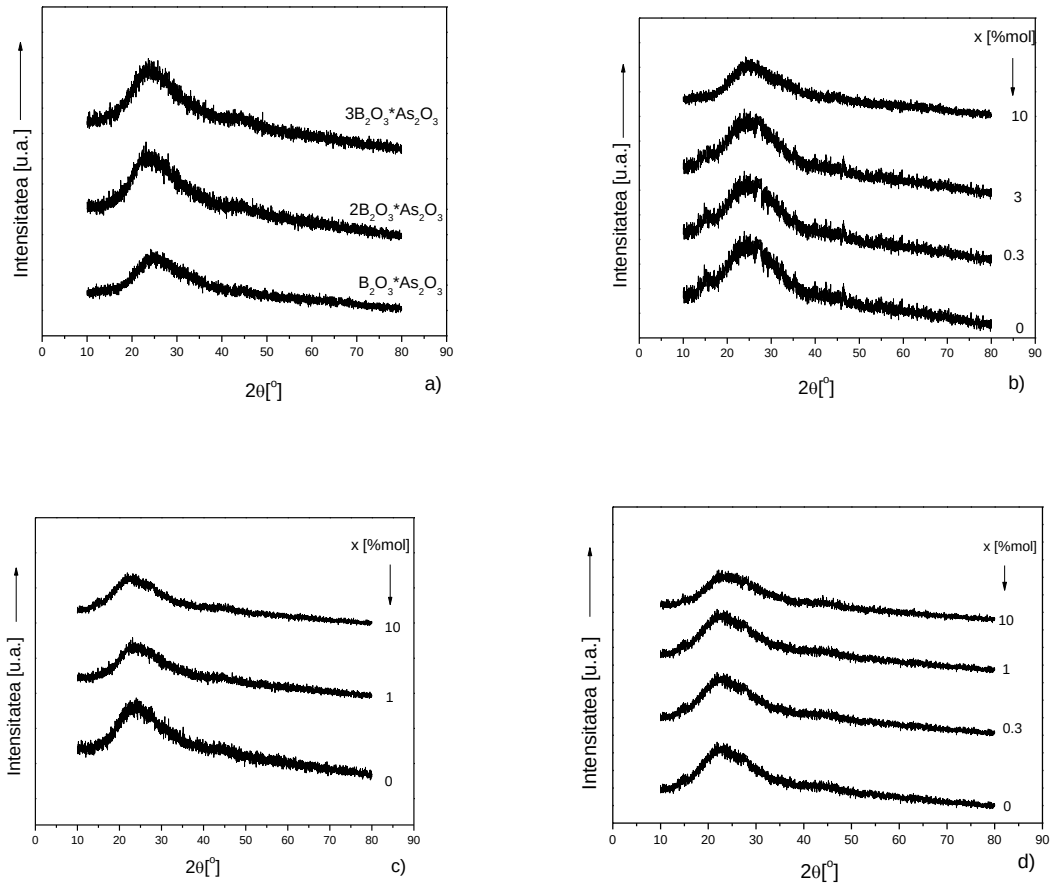

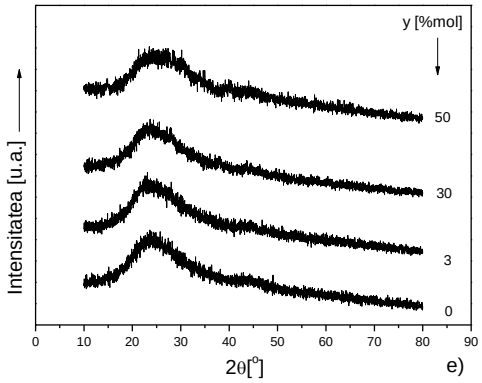

Fig. III.1.1. X-ray diffractograms of $xAg_2O\cdot(100-x)[zB_2O_3\cdot As_2O_3]$ with $0 \leq x \leq 10$ mol% and $z = 1; 2; 3$ – (a) ; (b) ; (c) ; (d) and $(1-y)Ag_2O\cdot yMnO\cdot 9[2B_2O_3\cdot As_2O_3]$ with $0 \leq y \leq 50$ mol% (e) system glasses

The FT – IR spectra have been recorded using a Bruker Equinox 55 with a spectral range from 4000 cm^{-1} to 370 cm^{-1}. A MIR, GLOBAR generator cooled with air was used. The detection was carried out with a DLATGS detector with a KBr window. The spectral resolution was about 0.5 cm^{-1}. The samples were prepared using KBr pellet technique.

Raman measurements were made with a Dilor Labram spectrometer (invers system, HRLabRam, Jobin Yvon Horiba) using using the 1064 nm line of a Nd/YAG laser. The power of the laser was 5 mW. The signal acquisition has been done using a CCD (Peltier CCD) and the soft was LabSpec 3.1. The spectra were obtained from 8 cycles of 30 seconds average, and the spectral resolution was 1 cm^{-1}.

The EPR spectra were obtained with an RPE Bruker ELEXSYS E500 in X-frequency band (9.4 GHz) and with a field modulation of 100 kHz. The measurements were from made at liquid nitrogen temperature to room temperature. The variable temperature unit was ER 4131VT type.

Magnetic susceptibility measurements were performed on a Faraday type balance in the 80 – 300 K temperature range.

Chapter VI

Results and discussions regarding the strucuture of vitreous oxide glasses from $xAg_2O\cdot(100-x)[zB_2O_3\cdot As_2O_3]$ with $0 \leq x \leq 10$ mol% and $z = 1; 2; 3$ and (1-

y)Ag_2O·yMnO·9[2B_2O_3·As_2O_3] with $0 \leq y \leq 50$ %mol with and $0 \leq y \leq 50$ mol% systems

IV.1. Comparative study of zB_2O_3·As_2O_3, with z = 1,2,3, matrice's structure

The vibration modes of borate glasses are active in three IR spectral zones: the first zone is from 600 to 800 cm^{-1} atributted to the bending vibrations of B-O-B linkages from various borate segments; the second region, 800-1150 cm^{-1}, is assigned to extension vibrations of B-O bonds from BO_4 units, and the third region, 1150-1550 cm^{-1}, is assigned to B-O and B-O^- bonds vibrations from BO_3 and BO_2O^- structural units.

The FT-IR absoption spectra of zB_2O_3·As_2O_3 matrices, with z = 1,2,3 are presented in figure IV.1.1 and the assignement of the absorption bands is presented in table IV.1. The interpretation of IR data has been made according to Tarte and Condrate theory [12,13] by comparing the experimental data with the data obtain for crystalline oxides.

In our case, the three mtrices presents similarities due to the big influence of formative oxide, B_2O_3.

The band from ~547 cm^{-1} is assigned to B–O–B bending vibrations in which are involved oxygen atoms from the exterior of boroxol rings [14] – its intensity is increasing with the increase of boron oxide concentration ; the band from ~606 cm^{-1} can be assigned to symmetric bending vibrations of As-O bonds [15], the band from ~644 cm^{-1} is assigned to bending vibrations of O–B–O bonds [15], its intensity is increasing with the increase of oron oxide concentration. The absorption band from ~805cm^{-1} is assigned to doubly degenerate stretching vibrations of As-O bonds [15] – its intensity is considerably increasing for the matrices with z = 2 and 3.

As for the second region, there are present four IR absorption bands, their intensity being small. The first band, from ~884 cm^{-1} and the band from ~1030 cm^{-1} are assigned to B-O bonds stretching vibrations in BO_4^- units from tri-, tetra- and penta-borate groups [16,17]. The band from ~926 cm^{-1} is assigned to B-O bonds stretching vibrations in BO_4 units from diborate groups [16,17], and the band from ~1118 cm^{-1} is assigned to asymmetric stretching vibrations of B-O bonds from

BO_4 units from different borate groups [12]. The intensity of these four bands is increasing with the increase of boron oxide concentration, especially for $B_2O_3 \cdot 2As_2O_3$ and $B_2O_3 \cdot 3As_2O_3$ matrices.

The absorption band from ~1196 cm^{-1} can be assigned to asymmetric stretching vibrations of B-O bonds in borate triangular units (BO_3 and BO_2O^-) from pyro- and ortho-borate groups [18], and the band from ~1459 cm^{-1} is assigned to B-O bonds stretching vibrations in BO_3 units from various borate groups. Their intensity is increasing with the increase of boron oxide concentration. In this region there is also present a weak infrared signal, shoulder-like, centered at ~1230 cm^{-1} and assigned to asymmetric stretching vibrations of B-O bonds from ortho-borate groups. As expected, with the increase of boron oxide concentration, all the bands assigned to borate structural units are increasing in intensity.

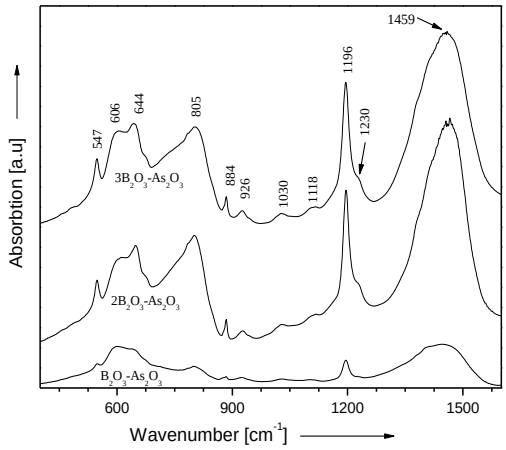

Fig. IV.2.1. FT-IR spectra of $zB_2O_3 \cdot As_2O_3$, where z = 1,2,3 matrices

To quantify the silver ions effect to the changes in the relative population of triangular and tetrahedral borate units we have calculated the integrated intensity of the absorption envelopes 850-1150 cm^{-1} and 1150 - 1500 cm^{-1} denoted by A_4 and A_3 respectively. A_4 and A_3 approximate the relative number of BO_4 and BO_3 units, respectively. The relative integrated intensity, $A_r = A_4/A_3$, is plotted in figure 2 versus Ag_2O content in figure IV.1.2. It can be observed that $A_r < 1$, which means that the predominant structural units in the studied glasses are BO_3 units. For $B_2O_3 \cdot 3As_2O_3$ matrice the value of A_r has a significant increase.

Table IV.1. Wavenumbers and band assignments of $zB_2O_3 \cdot As_2O_3$ where z = 1,2,3 matrices

$\tilde{\nu}$ (cm^{-1})	FT-IR assignments
~ 547	B–O–B bending vibrations in which are involved oxygen atoms from the exterior of boroxol rings
~ 606	Symmetric bending vibrations of As-O bonds
~ 644	Bending vibrations of O–B–O bonds
~ 805	Doubly degenerate stretching vibrations of As-O bonds
~ 884 ~ 1030	B-O bonds stretching vibrations in BO_4^- units from tri-, tetra- and penta-borate groups
~ 926	B-O bonds stretching vibrations in BO_4 units from diborate groups
~ 1118	Asymmetric stretching vibrations of B-O bonds from BO_4 units from different borate groups
~ 1196	Asymmetric stretching vibrations of B-O bonds in borate triangular units (BO_3 and BO_2O^-) from pyro- and ortho-borate groups
~ 1230	Asymmetric stretching vibrations of B-O bonds from ortho-borate groups
~ 1459	Stretching vibrations in BO_3 units from various borate groups

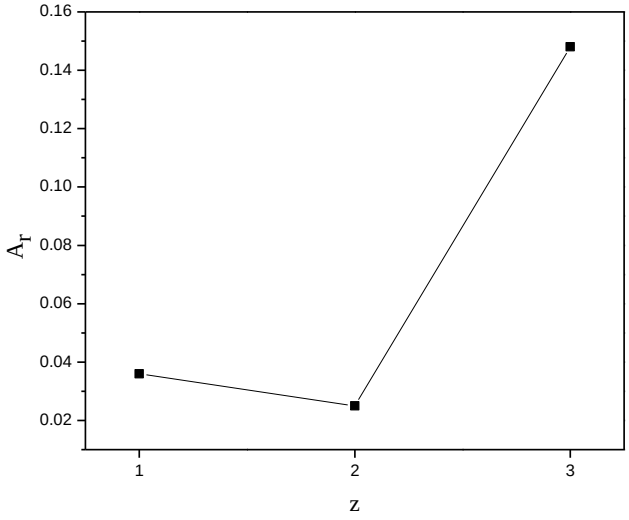

Fig. IV.2.2. A_r ratio as a function of B_2O_3 concentration for $zB_2O_3 \cdot As_2O_3$, where z = 1,2,3 matrices

In figure IV.1.3. is presented the Raman spectra for $zB_2O_3 \cdot As_2O_3$, with z = 1,2,3 matrices and their assignement is presented in table IV.2.

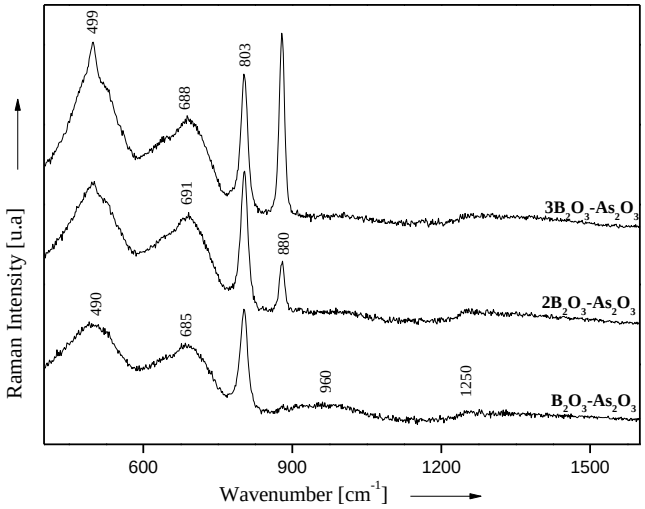

Fig. IV.2.3. Raman spectra of $zB_2O_3 \cdot As_2O_3$, where z = 1,2,3 matrices

The increase of boron oxid concentration induces structural changes in studied matrices. The bands from ~490 cm^{-1} and the band from ~685 cm^{-1}, assigned to vibrations of isolated di–borate groups and/or vibrations of As-O bonds and to vibrations of chain and/or ring type meta- and penta- borate groups increase in intensity for high boron content matrices, which leads to an increase of di-borate and meta-, and penta-borate groups. The band from ~803 cm^{-1} is assigned to symmetric breathing vibrations of boroxol rings and is predominant for z = 1,2 matrices. The band from ~880 cm^{-1} is assigned to vibrations of ortho-borate groups and appears for z = 2 and 3 matrices. For the matrice with z = 3 this band increases in intensity and becomes the predominant band in the spectra. The weak Raman signal from ~960 cm^{-1} is assigned to vibrations of ortho-borate groups and appears for z = 1 matrice. The broad band from ~1250 cm^{-1} is assigned to vibrations of pyro-borate groups.

Table IV.2. Wavenumbers and Raman band assignments of $zB_2O_3 \cdot As_2O_3$ where z = 1,2,3 matrices

$\tilde{\nu}$ (cm^{-1})	Raman assignments
~490	Vibrations of isolated di–borate groups and/or vibrations of As-O bonds
~685	Vibrations of chain and/or ring type meta- and penta- borate groups
~803	Symmetric breathing vibrations of boroxol rings
~880	Vibrations of ortho-borate groups
~960	Vibrations of ortho-borate groups
~1250	Vibrations of pyro-borate groups

IV.2. The study by infrared absorption spectroscopy of glasses from $xAg_2O \cdot (100-x)[zB_2O_3 \cdot As_2O_3]$ with $0 \leq x \leq 10$ mol% and z = 1; 2; 3 and $(1-y)Ag_2O \cdot yMnO \cdot 9[2B_2O_3 \cdot As_2O_3]$ with $0 \leq y \leq 50$ %mol with and $0 \leq y \leq 50$ mol% systems

The FT-IR spectra characteristic to $xAg_2O \cdot (100-x)[zB_2O_3 \cdot As_2O_3]$, with $0 \leq x \leq 10$ mol% and z = 1,2,3 are presented in figure IV.2.1(a,b,c), and the bands assignement is presentd in table IV.3.

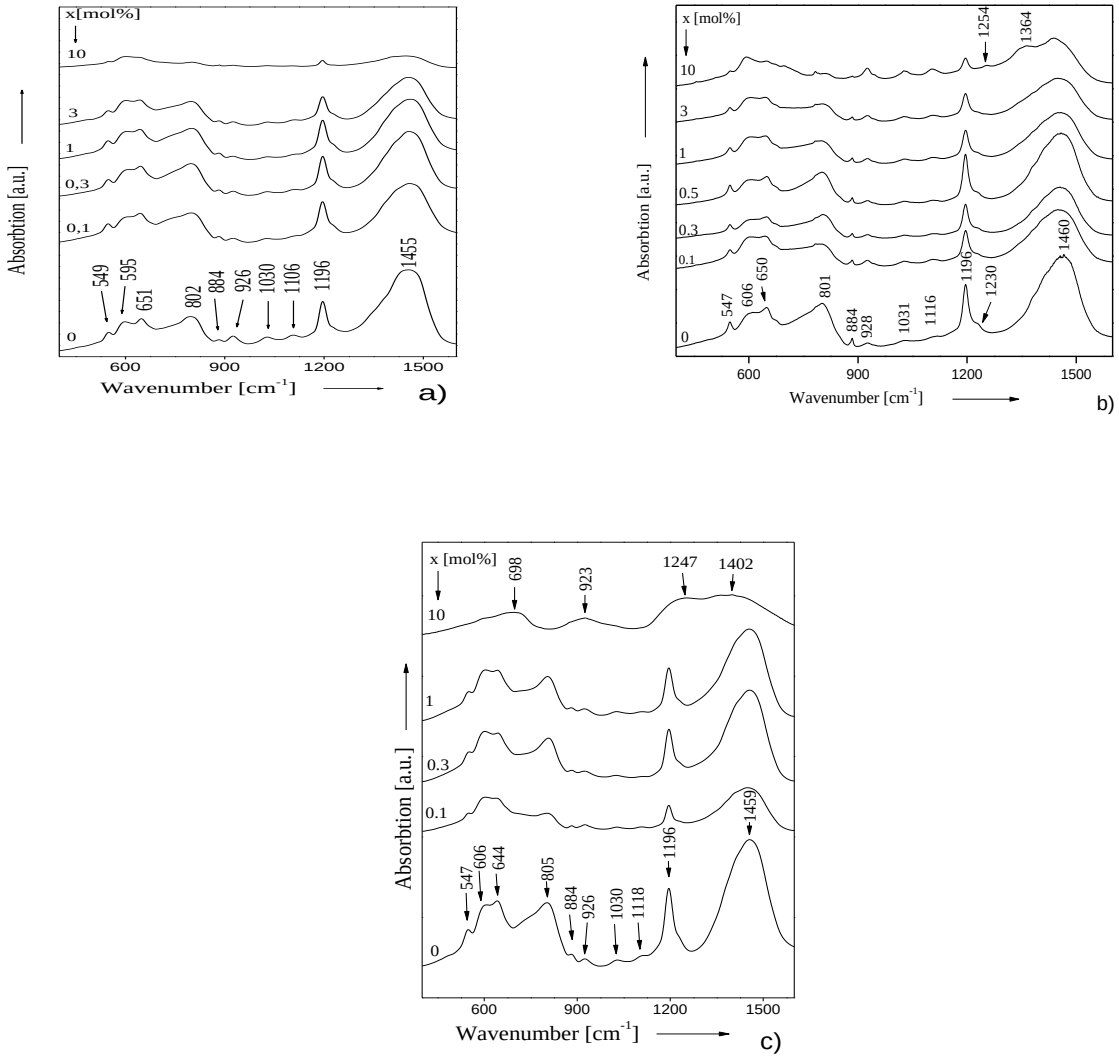

Fig. IV.2.1. FT-IR spectra of

$xAg_2O\cdot(1-x)[zB_2O_3\cdot As_2O_3]$, with $0 \leq x \leq 10$ mol% and z = 1,2,3 glass systems

The structure proposed for $xAg_2O\cdot(100-x)[zB_2O_3\cdot As_2O_3]$ with $0 \leq x \leq 10$ mol% and z = 1,2,3 matrices from FT-IR measurements consists of di-, tri-, tetra-, penta- , piro- and orto-borate, as from structural units characteristic to arsen oxide. With the addition and the increase of silver oxide content, the intensity of the bands is decreasing and they become broadened.

The bands from ~1230 and ~1364 cm^{-1} present in xAg2O·(1-x)[$2B_2O_3$·As_2O_3] system are assigned to asymmetric streching vibrations of B-O bonds from ortho-borate groups and to streching vibrations of B-O bonds from BO_3 units from different borat groups.

Table IV.3. Wavenumbers and FT-IR bands assignment of $xAg_2O·(1-x)[zB_2O_3·As_2O_3]$, with $0 \leq x \leq 10$ mol% and z = 1,2,3 systems

$\tilde{\nu}$ (cm^{-1})			Assignment
$xAg_2O·(100-x)[zB_2O_3·As_2O_3]$			
z = 1	z = 2	z = 3	
~ 549	~ 547	~ 547	B–O–B bonds bending vibrations involving oxygen atoms outside borate rings
~ 595	~ 606	~ 606	Symmetric bending vibrations of As – O bonds
~ 651	~ 650	~ 644	O–B–O bonds bending vibrations
~ 802	~ 801	~ 805	Doubly degenerate stretching vibrations of As-O bonds
~ 884 ~ 1030	~ 884 ~ 1031	~ 884 ~ 1031	B-O bonds stretching vibrations in BO_4^- units from tri-, tetra- and penta-borate groups
~ 926	~ 928	~ 926	B-O bonds stretching vibrations in BO_4 units from diborate groups
~ 1106	~ 1116	~ 1118	Asymmetric stretching vibrations of B-O bonds from BO_4 units
~ 1196	~ 1196	~ 1196	Asymmetric stretching vibrations of B- bonds in borate triungular units (BO_3 and BO_2O^-) from pyro- and ortho-borate groups
	~ 1230		Asymmetric stretching vibrations of B-O bonds from ortho-borate groups
~ 1455	~ 1460	~ 1459	B-O bonds stretching vibrations in BO_3 units from various borate groups

For xAg2O·(1-x)[$3B_2O_3$·As_2O_3] system and for high silver concentrations, two absorption bands appear at la ~1247 and ~1364 cm^{-1} assigned to asymmetric streching vibrations of B-O bonds from ortho-borate groups and to streching vibrations of B-O bonds in BO_3 units from different borate groups.

In figure IV.3.2 (a,b,c) is presented the dependence of $A_r = A_4/ A_3$ versus silver oxide concentration for $xAg_2O·(100-x)[zB_2O_3·As_2O_3]$ with $0 \leq x \leq 10$ mol% and z = 1,2,3 glass systems. For the system with z = 1 the value of A_r decreases for $x \leq 3$ mol%, and for x > 3 mol% the value of A_r is increasing. That indicates the fact that forming of structural units in which boron atoms are tri-coordinated is favourized up to x = 3 mol%, and for higher concentrations the forming of structural units in which boron atoms are tetra-coordinated is favourized [22]. For the other two systems, the value of A_r increases for all studied concentrations.

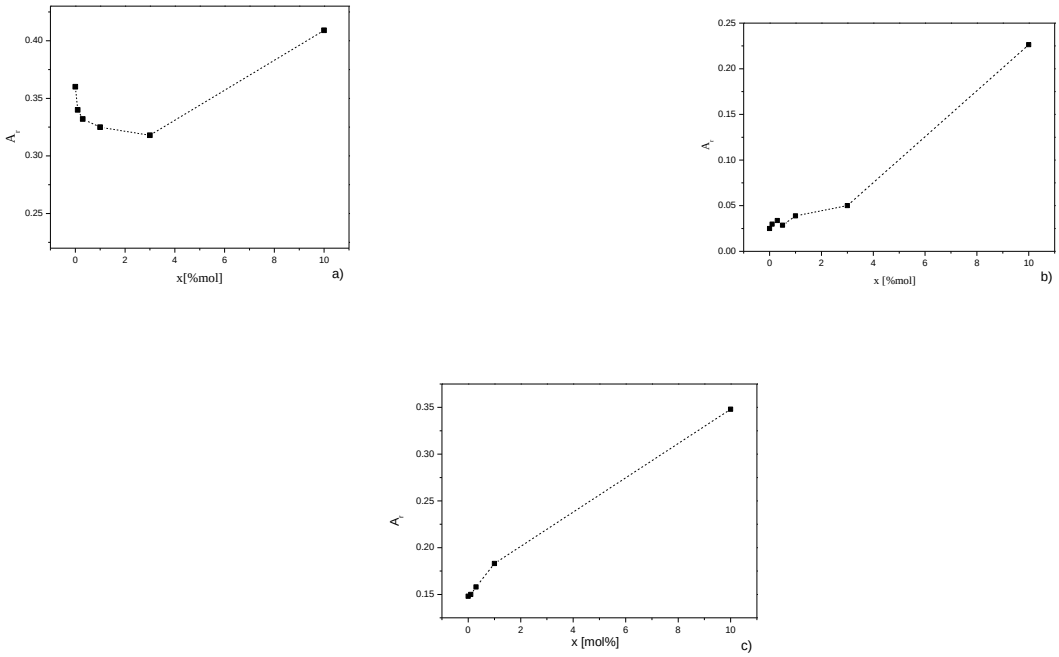

Fig. IV.3.2. A_r ratio as a function of Ag_2O content in $xAg_2O·(100-x)[zB_2O_3·As_2O_3]$, with $0 \leq x \leq 10$ mol% and z = 1,2,3 (a,b,c) glass systems

Like figure IV.3.3 shows, the addition of manganese ions has as effect the intensity decrease for all absorption bands present in the spectra, so we can conclude that the disorder of the structure increases with the increase of manganese ions content. For the sample with the higher manganese

ions content, the spectra contains five low intensity and broaden: ~570, ~760, ~940, ~1100 and ~1270 cm^{-1}. The assignement of these bands is presented in IV.4.

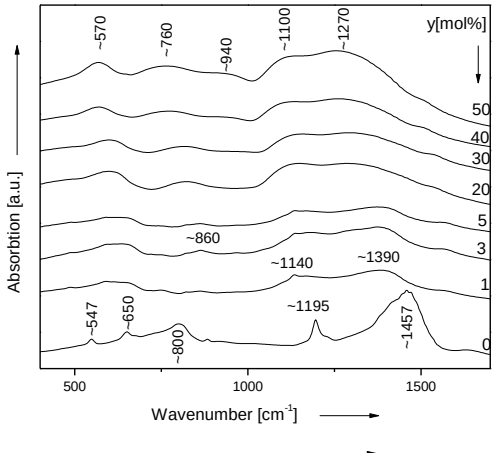

Fig. IV.3.3. FT-IR spectra of $x[(1-y)Ag_2O{\cdot}yMnO]{\cdot}(100-x)[2B_2O_3{\cdot}As_2O_3]$, with x = 10 mol% and $0 \leq y \leq 50$ mol% glass system

Table IV.4. Wavenumbers and FT-IR bands assignment of $x[(1-y)Ag_2O{\cdot}yMnO]{\cdot}(100-x)[2B_2O_3{\cdot}As_2O_3]$, with x = 10 mol% and $0 \leq y \leq 50$ mol% glass system

$\tilde{\nu}$ (cm^{-1})	Assignment
~ 547	B–O–B bonds bending vibrations involving oxygen atoms outside borate rings
~ 650	O–B–O bonds bending vibrations
~ 760	Bending vibrations of $O_3B - O - BO_4$ bonds
~ 883	B-O bonds stretching vibrations in BO_4^- units from tri-, tetra- and penta-borate groups
~ 940	B-O bonds stretching vibrations in BO_4 units from diborate groups
~ 1100	Asymmetric stretching vibrations of B-O bonds from BO_4 units from tri-, tetra- and penta-borate groups
~ 1270	Asymmetric stretching vibrations of B-O bonds from ortho-borate groups

~ 1195	Asymmetric stretching vibrations of B- bonds in borate triungular units (BO_3 and BO_2O^-) from pyro- and ortho-borate groups
~ 1457	B-O bonds stretching vibrations in BO_3 units from various borate groups

The evolution of A_r with the increase of manganese ions content is presented in figure IV.3.4. The value of A_r increases for $y \geq 3$ mol% and than decreases for for $3 \leq y \leq 5$ mol% with a high gradient. For manganese ions concentrations higher than y = 5 mol%, the value of A_r proportion continues to decrease, but with a smaller gradient. For $y \leq 3$ mol%, the increase of manganese ions content favourizes the transformation of tri-coordinated boron atoms in tetra-coordonated ones, and for y > 3 mol% the increase of manganese ions content favourizes the formation of structural units in which boron atoms are tri-coordinated, leading to network depolimerization [23].

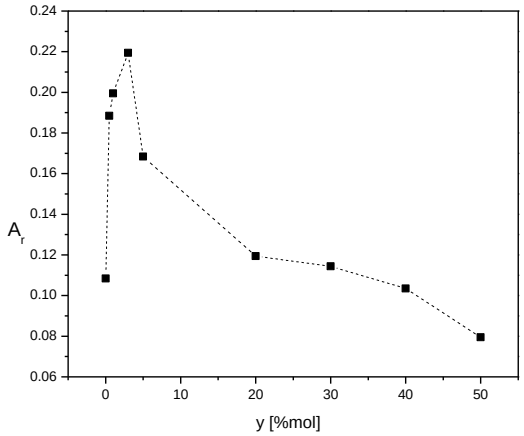

Fig. IV.3.4. A_r ratio as a function of $x[(1-y)Ag_2O \cdot yMnO] \cdot (100-x)[2B_2O_3 \cdot As_2O_3]$ with x = 10 mol% and $0 \leq y \leq 50$ mol% glass system

IV.4. The study by Raman spectroscopy of glasses from $xAg_2O\cdot(100-x)[zB_2O_3\cdot As_2O_3]$ with $0 \leq x \leq 10$ mol% and z = 1; 2; 3 and $x[(1-y)Ag_2O\cdot yMnO]\cdot(100-x)[2B_2O_3\cdot As_2O_3]$ with x = 10 mol% and $0 \leq y \leq 50$ mol% systems

In figure IV.4.1 are presented the Raman spectra for $xAg_2O\cdot(1-x)[zB_2O_3\cdot As_2O_3]$, with $0 \leq x \leq 10$ mol% and z = 1,2,3 glass systems, and table IV.5 presents the assignement of Raman bands evidenced in the spectra.

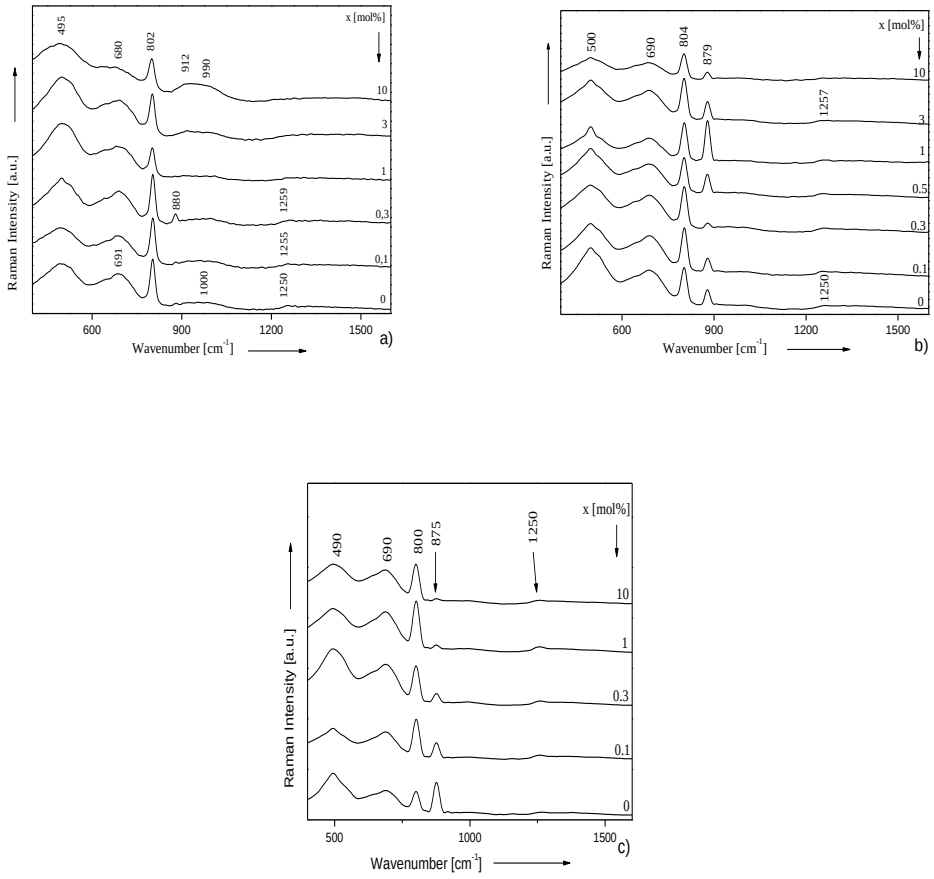

Fig. IV.4.1. Raman spectra of $xAg_2O\cdot(1-x)[zB_2O_3\cdot As_2O_3]$, with $0 \leq x \leq 10$ mol% and z = 1,2,3 glass systems

The predominant bands in Raman spectra characteristic to $xAg_2O\cdot(1-x)[zB_2O_3\cdot As_2O_3]$, with $0 \leq x \leq 10$ mol% and z = 1,2,3 glass systems are the ones situated at ~490, ~690 ş i ~802 cm^{-1}. For $xAg_2O\cdot(1-x)[zB_2O_3\cdot As_2O_3]$, with z = 2 and 3 glass systems, in the Raman spectra there is present a band situated at ~880 cm^{-1} for all studied concentrations.

The structural changes due to the introduction and the addition of manganese ions, from the Raman spectroscopy point of view, and characteristics to $x[(1-y)Ag_2O \cdot yMnO] \cdot (100-x)[2B_2O_3 \cdot As_2O_3]$ glass system are presented in figure IV.4.2, and the assignement of these bands are presented in table IV.6.

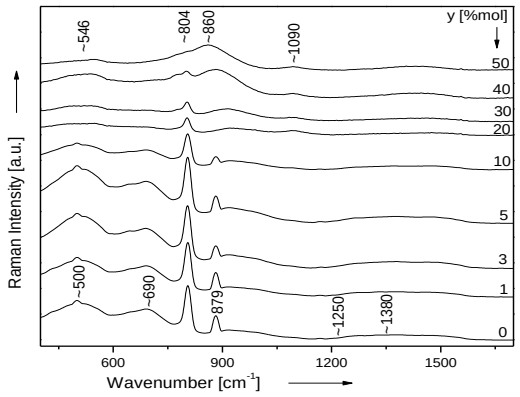

Fig. IV.4.2. Raman spectra of $x[(1-y)Ag_2O \cdot yMnO] \cdot (100-x)[2B_2O_3 \cdot As_2O_3]$, with x = 10 mol% and $0 \leq y \leq 50$ mol% glass system

Tabelul IV.5. Wavenumbers and Raman bands assignement of $xAg_2O \cdot (1-x)[zB_2O_3 \cdot As_2O_3]$, with $0 \leq x \leq 10$ mol% and z = 1,2,3 glass systems

$\widetilde{\nu}$ (cm^{-1})			Assignement
$xAg_2O \cdot (1-x)[zB_2O_3 \cdot As_2O_3]$			
z = 1	z = 2	z = 3	
~ 495	~ 500	~ 490	Vibrations of isolated di–borate groups and/or vibrations of As-O bonds
~ 691	~ 690	~ 690	Vibrations of chain and/or ring type meta- and penta- borate groups
~ 802	~ 804	~ 800	Symmetric breathing vibrations of boroxol rings
~ 880	~ 879	~ 875	Vibrations of ortho-borate groups
~ 1000			Vibrations of ortho-borate groups
~1250	~1250	~1250	Vibrations of pyro-borate groups

Tabelul IV.6. Wavenumbers and Raman bands assignement of $x[(1-y)Ag_2O \cdot yMnO] \cdot (100-x)[2B_2O_3 \cdot As_2O_3]$, with x = 10 mol% and $0 \leq y \leq 50$ mol% glass system

$\tilde{\nu}$ (cm^{-1})	Assignement
~ 500	Vibrations of isolated di–borate groups and/or vibrations of As-O bonds
~ 690	Vibrations of chain and/or ring type meta- and penta- borate groups
~ 804	Symmetric breathing vibrations of boroxol rings
~ 879	Vibrations of ortho-borate groups
~ 1090	Vibrations of di-borate groups formed of six-member rings BO_4 tetrahedra
~1250	Vibrations of pyro-borate groups
~1380	Streching vibrations of $B–O^-$ bonds in BO_4 from diferent borate groups

The increase of manganese ions content leads to th appearance in Raman spectra, starting with y = 20 mol% concentration, of a low intensity band centered at ~1090 cm^{-1}, which is assigned to vibrations of di-borate groups formed of six-member rings BO_4 tetrahedra [24]. For higher manganese concentrations the predominant band in the Raman spectra is the broaden band from ~879 cm^{-1}. From Raman investigations we can conclude that the adding of manganese ions into $xAg_2O \cdot (1-x)[2B_2O_3 \cdot As_2O_3]$ vitreous matrix leads to structural modifications and to the increase of disorder degree, especially for higher manganese ions concentrations ($y \geq 20$ %mol).

IV.5. Magnetic behavior of glasses from $x[(1-y)Ag_2O \cdot yMnO] \cdot (100-x)[2B_2O_3 \cdot As_2O_3]$ system

The manetic behaviour of $x[(1-y)Ag_2O \cdot yMnO] \cdot (100-x)[2B_2O_3 \cdot As_2O_3]$, with x = 10 mol% and $0 \leq y \leq 50$ mol% glass system has been investigated in the 80÷300K temperature range (figure IV.5.1.a,b).

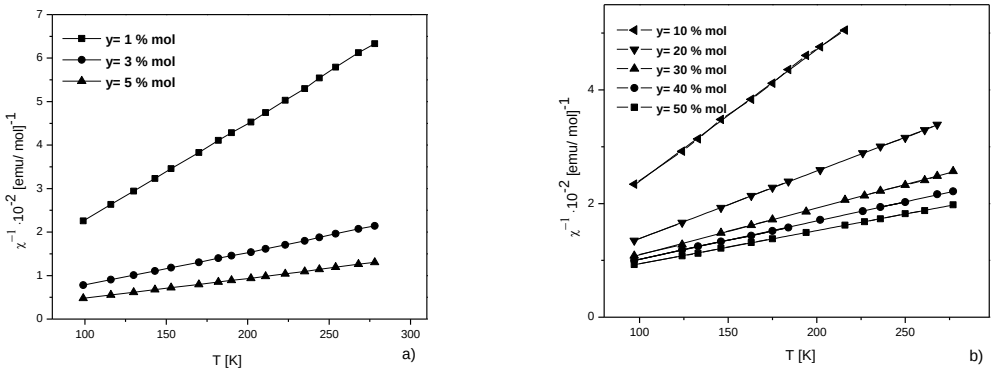

Fig. IV.5.1.a,b - Temperature dependence of χ^{-1} for x[(1-y)Ag_2O·yMnO]·(100-x)[$2B_2O_3$·As_2O_3], with x = 10 mol% and $0 \leq y \leq 50$ mol% glass system

For $y \leq 5$ %mol the x[(1-y)Ag_2O·yMnO]·(100-x)[$2B_2O_3$·As_2O_3] glass system presents a paramagnetic behaviour and the temperature dependence of the reciprocal magnetic susceptibility obeys a Curie law, suggesting that in $0 \leq y$ 5 %mol compositional range the manganese ions are isolated and/or they participate in dipol – dipol interactions.

For manganese ions concentrations higher than 5 mol% the temperature dependence of the reciprocal magnetic susceptibility obeys (fig. IV.5.1.b) a Curie-Weiss law, with negative paramagnetic Curie temperature (θ_p); its value depending on the concentration of manganese ions. This dependence suggests that for manganese ions concentrations higher than 5 mol%, the manganese ions participate in superexchange interactions characteristic to antiferromagnetic coupled ions by means of superexchange interactions.

Analyzing the manganese ions concentration dependence of paramagnetic Curie temperature of all investigated samples (fig. IV.5.2.), it can be concluded that this dependence is relatively zero for $y \leq 5$ mol%. For concentrations higher than 5 mol% the absolute value of paramagnetic Curie temperature increases linearly with the increase of manganese ions content, indicating the increase of superexchange interactions. These interactions are the narrowing mechanisms of EPR resonance line from $g_{eff} \approx 2.0$ and explains the gradient change of $\Delta B = f(y)$ curve (fig. IV.6.2.a).

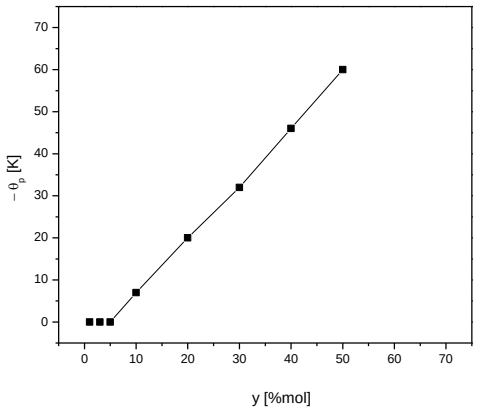

Fig. IV.5.2. Concentration dependence of θ_p for x[(1-y)Ag_2O·yMnO]·(100-x)[$2B_2O_3$·As_2O_3] glass system

In table IV.7 are presented the values of Curie molar constants, effective magnetic moments and molar fractions characteristic to $Mn^{2+}(y_1)$ şi $Mn^{3+}(y_2)$ ions.

The values of molar fractions y_1 and y_2 characteristic to $Mn^{2+}(y_1)$ şi $Mn^{3+}(y_2)$ ions increase with the increase of manganese ions content up to y = 30 mol%. Over this concentration, the values of molar fraction characteristic to Mn^{2+} ions is decreasing, becoming predominant the molar fraction characteristic to Mn^{3+} ions.

Tabelul IV.7. Molar Curie constants, effective magnetic moments and molar fractions of $Mn^{2+}(y_1)$ and $Mn^{3+}(y_2)$ for x[(1-y)Ag_2O·yMnO]·(100-x)[$2B_2O_3$·As_2O_3] glass system

y [mol% MnO]	C_M [emu/ mol]	μ_{ef} [μ_B]	y_1 [mol% $Mn^{2+}O$]	y_2 [mol% $Mn^{3+}O$]
1	11,56	5,92	1	-
3	13,34	5,90	2,93	0,07
5	20,25	5,88	4,78	0,22
10	43,15	5,87	9,47	0, 53
20	83,96	5,79	17,25	2,75

30	119,04	5,63	20,9	9,1
40	144,92	5,38	17,89	22,11
50	171,23	5,23	15,15	34,85

IV.6. The study by EPR of glasses from $x[(1-y)Ag_2O \cdot yMnO] \cdot (100-x)[2B_2O_3 \cdot As_2O_3]$ glass system

In order to obtain more information regarding the behaviour of manganese ions in vitreous matrices, the $x[(1-y)Ag_2O \cdot yMnO] \cdot (100-x)[2B_2O_3 \cdot As_2O_3]$ glass system was investigated through means of electron paramagnetic resonance (EPR) in a compositional range of $0 \leq y \leq 50$ mol% of manganese ions.

The EPR spectra obtain at room temperature are prsented in figure IV.6.1.a and b. Superimposed on $g_{eff} \approx 4.3$ absorption line the narrowline corresponding to accidental impurities of Fe^{3+} ions was also detected for $y \leq 5$ mol% [30].

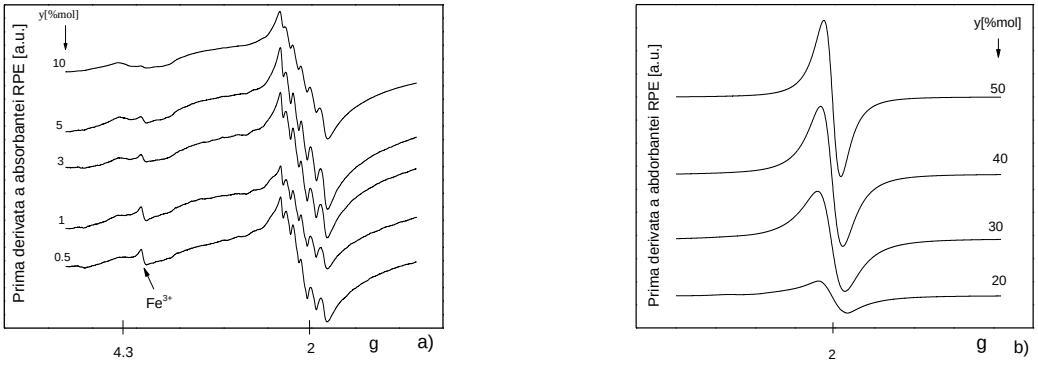

Fig. IV.6.1. EPR spectra of $x[(1-y)Ag_2O \cdot yMnO] \cdot (100-x)[2B_2O_3 \cdot As_2O_3]$, with $0,5 \leq y \leq 10$ mol% (a) and with $20 \leq y \leq 50$ mol% (b)

In EPR spectra, the predominant line is the resonance line centered at $g_{eff} \approx 2$, showing hfs characteristic of the ^{55}Mn (I = 5/2) isotope. The hyperfine sextet situated at $g_{eff} \approx 2,0$ is characteristic to isolated Mn^{2+} ions situated in high symmetric octahedral sites, having approximately the same microvicinity structure.

From the $g_{eff} \approx 2,0$ (fig.IV.6.2.a) line-width evolution it can be observed that its value increases linear up to y = 5 %mol, than up to y = 20 mol% is increasing, but with smaller gradient and for higher manganse ions content the value of line-width is decreasing. From this observation we can conclude that up to y = 5 %mol between Mn^{2+} there are present dipolar interactions, as predominant mechanism for the width of the resonance line. The decrease of the gradient for $5 < y \leq 20$ mol%, indicates that in this compositional range the Mn^{2+} ions participate, besides in dipolar interactions, in magnetic superexchange interactions. For concentrations higher than 20 mol% the resonance line narrows indicating the fact that the Mn^{2+} ions participate only in magnetic superexchange interactions. The intensity of the resonance line from $g_{eff} \approx 2,0$ increases up to y = 40 mol%, and for higher manganese ions content is decreasing, suggesting the fact that in network there are present also manganese ions in 3+ valence state [25,26].

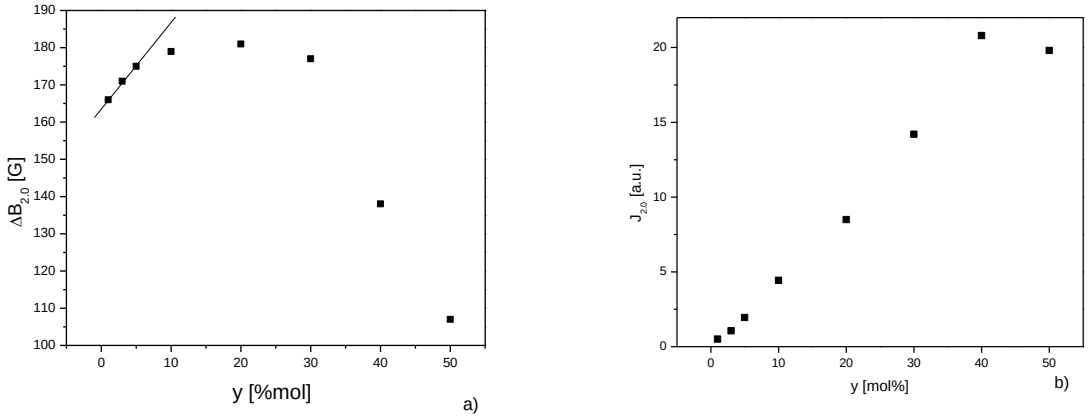

Fig. IV.6.2. Composition dependence of the line intensity (a) and the line–width (b) of EPR absorption at $g_{eff} \approx 4.3$

In EPR spectra of small manganese ions content ($y \leq 10$ %mol) is present the resonance line centered at $g_{eff} \approx 4,3$, characteristic to isolated manganese ions disposed in cubic symmetric sites slightly tetragonally or rhombically distorted [27] (fig. IV.6.1)

The intensity of this line increases up to y = 5 mol% due to the increase of Mn^{2+} ions. For higher mangense ions concentrations the intensity of this line decreases due to the modifications in Mn^{2+} ions vicinities configurations, and they do not assure any longer the magnetic isolation of

Mn^{2+} ions. The evolution of line-width for $g_{eff} \approx 4,3$ resonance line follows the evolution of its intensity, so up to 5 mol% manganese ions the line-width increases due to the increase of Mn^{2+} ions number, and than decreases (fig. IV.6.3.).

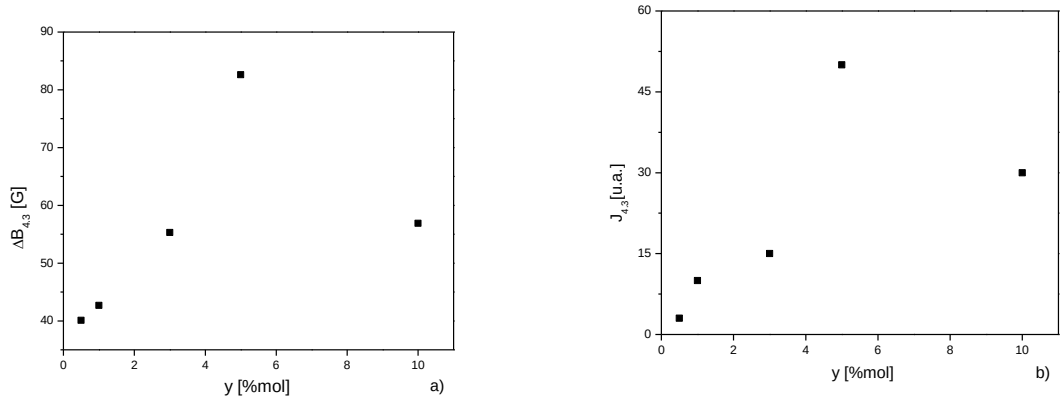

Fig. IV.6.3. Composition dependence of the line intensity (a) and the line–width (b) of EPR absorption at g ≈ 4,3

Selective references

[I.1.] D.Becherescu, V.Cristea, F.Marx, I.Menessz, F.Winter, Chimia stării solide, Ed. Şt. Enc., Buc., vol. 1, 1983;

[I.2.] I. Ardelean, Introducere în studiul materialelor oxidice cu structură vitroasă, Ed. Napoca Star, Cluj-Napoca, 2002;

[I.3.]D.R.Uhlmann, R.R.Shaw, J. Non-Cryst. Solids, 1, 347 (1969);

[I.4.] W.L.Konijnendijk, J.M.Stevels, J. Non-Cryst. Solids, 18, 307 (1975);

[I.5.] B.N.Meera, J. Ramakrishna, J. Non-Cryst. Solids, 159, 1 (1993);

[I. 6.] Al.Nicula, M.Peteanu, Studia Univ. Babeş -Bolyai, Physica XXI, 42 (1976);

[I. 7.] E.Burzo, I.Ardelean, I.Ursu, J. Mat. Sci., 15, 581 (1980);

[I. 8] I.Ardelean, M.Peteanu, S.Simon, V.Simon, F.Ciorcaş , C.Bob, S.Filip, Indian J. Phys., 74A (5), 467 (2000);

[I. 9.] R.Ciceo-Lucăcel, I.Ardelean, Int. J. Mod. Phys. B, 18(20/21), 2915 (2004);

[I.10.] Gh.Ilonca, I.Ardelean, O.Cozar, J. Magn. Magn. Mat., 54-57, 223 (1986);

[II.11.] A. Gale, A.K. Jain, L. Vallow, Int. J. Radiation Oncology-Biology-Physics, 69, 3 (2007);

[IV.12.] P. Tarte, Spectrochim. Acta 18, 467 (1962);

[IV.13.] R. A. Condrate, J. Non – Cryst. Solids 84, 26 (1986);

[IV.14.] J. F. Ducel, J. J. Videau, M. Couzi, Phys. Chem. Glasses 34, 212, (1993);

[IV.15.] G. Srinivisarao , N. Veeraiah , J. Alloys Compounds 327, 52, (2001);

[IV.16.] E. I. Kamitsos, M. A. Karakassides, G. D. Chryssikos, J. Phys. Chem. 91, 1073, (1987);

[IV.17.] E.I. Kamitsos, M. A. Karakassides and G.D. Chyssikos, Phys. Chem. Glasses, 30, 229 (1989);

[IV.18.] Y.D.Yiannopoulos, G.D.Chryssikos and E.I.Kamitsos, Phys. Chem. Glasses, 42 (3), 164 (2001);

[IV.19.] M. M. El-Desoky, H. Farouk, A. M. Abdalla and M. Y. Hassaan, J. Mat. Sci.: Mat. Electronics, 9, 77 (1998);

[IV.20.] I.Ardelean, M. Peteanu, R. Ciceo-Lucăcel and I. Bratu, J. Mat. Sci.: Mat. Electronics, 11, 11 (2000);

[IV.21.] I. Bratu. I. Ardelean and R. Ciceo-Lucăcel**,** Rom. Rep. Phys., Vol. 51, 7-10, 955, (1999);

[IV.22.] ***S.C. Baidoc*** ș i I. Ardelean, Modern Physics Letters B, 24, 1, 51, (2010);

[IV.23.] ***Sergiu C. Baidoc,*** I. Ardelean, Petru Pascuta, Physica B: Condensed Matter, 406, 4253, (2011);

[IV.24.] J.C. Sabadel, P. Armand, D. Cachau-Herreillat, P. Baldeck, O. Doclot, A. Ibanez and E. Philippot, J. Solid State Chem., 132, 411 (1997);

[IV.25.] V. Timar ș i I. Ardelean, JOAM, 10, (12), 3212, (2008);

[IV.26.] I. Ardelean, M. Peteanu, R. Ciceo – Lucăcel, "Studii de rezonanță paramagnetică electronică şi magnetice ale unor ioni 3d în sticlele pe bază de B_2O_3", Presa Universitară Clujeană, Cluj-Napoca, 2005;

[IV.27.] I. Ardelean, M. Peteanu, Gh. Ilonca, Phys. Stat. Sol. (a), 58, K33, (1980);

Selected conclusions

The paper presents the experimntal results obtain for the samples from the systems: $xAg_2O\cdot(100-x)[zB_2O_3\cdot As_2O_3]$ with $0 \leq x \leq 10$ mol% and z = 1; 2; 3, respectively from $x[(1-y)Ag_2O\cdot yMnO]\cdot(100-x)[2B_2O_3\cdot As_2O_3]$ with x = 10 mol% and $0 \leq y \leq 50$ mol%.

For a more accurate comparative study of the above mentioned systems, these were prepared in the same conditions (the melting oven, the crucibles, the melting temperature and the melting time were the same). The investigation methods used are X-ray diffraction, FT-IR spectroscopy, Raman spectroscopy, electron paramagnetic resonance (EPR) and magnetic susceptibility measurements.

From the X-ray diffraction measurements made on the samples from the above mentioned systems, it can be concluded that homogenous oxidic glasses were formed through out the entire Ag_2O and MnO concentrations range.

From the FT-IR and Raman spectra of the investigated samples it can be concluded that:

1. In the structure of the system's matrices the predominant structural units are those in which boron atoms are tri-coordinated.
2. FT-IR spectroscopy evidenced the presence of boron oxide characteristic structural units (di-, tri-, tetra-, penta-, ortho- and piro-borate groups) and also the presence of arsenic oxide (As-O bonds).
3. The structure of the investigated systems changes with the progresive addition of Ag_2O.
4. The addition of MnO in the $x[(1-y)Ag_2O\cdot yMnO]\cdot(100-x)[2B_2O_3\cdot As_2O_3]$ system leads to increasing of disorder degree in the structure of the studied samples.
5. The presence of the silver oxide has not been evidenced for any studied system, not by FT-IR spectroscopy and not by Raman spectroscopy.
6. The values of the A_r ratio indicates that the predominant structural units for all the investigated systems are those in which boron atoms are tri-coordinated.

From the electron paramagnetic resonance and magentic susceptibility measurements done for the samples from the $x[(1-y)Ag_2O \cdot yMnO] \cdot (100-x)[2B_2O_3 \cdot As_2O_3]$ system, it can be concluded that:

- The EPR spectra are characteristic to Mn^{2+} ions and are formed from the resonance lines centered at $g_{eff} \approx 4,3$ and $g_{eff} \approx 2,0$.
- The resonance line centers at $_{geff} \approx 4,3$ is typical for isolated Mn^{2+} ions disposed in cubic symmetric sites slightly tetragonally or rhombically distorted.
- The $g_{eff} \approx 2.0$ resonance absorption line can be assigned to isolated manganese ions as well as to those implicated in dipolar or/and super-exchange magnetic interactions.
- The evolution of the ΔB and J parameters is typical for manganese ions involved in dipolar or/and super-exchange magnetic interactions.
- Magnetic properties of the investigated samples depends on the manganese ions content.
- The increasing ot the molar Curie constant with the increase of MnO concentration explains the increasing of the paramagnetic ions content.